

Supporting Information for "In silico discovery of active, stable, CO-tolerant and cost-effective electrocatalysts for hydrogen evolution and oxidation"

Seoin Back,^{*,†,§} Jonggeol Na,^{‡,§} Kevin Tran,[¶] and Zachary W. Ulissi^{*,¶}

[†]*Department of Chemical and Biomolecular Engineering, Sogang University, Seoul 04107,
Republic of Korea*

[‡]*Division of Chemical Engineering and Materials Science, Ewha Womans University, Seoul
03760, Republic of Korea; E-mail: jgna@ewha.ac.kr*

[¶]*Department of Chemical Engineering, Carnegie Mellon University, Pittsburgh, PA, USA*

[§]*These authors contributed equally to this work.*

E-mail: sback@sogang.ac.kr; zulissi@andrew.cmu.edu

Methods

We collected the data from open-source DFT database for adsorption calculations, *GASpy*.¹ When generating data, we first collected 1,499 intermetallic crystals from Materials Project² and modelled surfaces with Miller indices between -2 and 2, inclusively, which results in 17,507 surface structures. One surface could have several unique sites for adsorption, for example, top, bridge, FCC-three-fold hollow, HCP-three-fold hollow and four-fold hollow site. The number of active sites is even more for surfaces consisting of multi-elements. For those structures, 1,684,908 unique active sites were found. We calculated binding energies at all unique sites and used the most stable one to evaluate catalytic properties since the most strongly binding surface sites are most likely to contribute to the reactions. DFT calculations were performed using VASP code^{3,4} with GGA-RPBE⁵ exchange-correlation functional and projector augmented wave (PAW) pseudopotential.⁶ Bulk relaxations were performed to obtain RPBE-level lattice parameters, and atomic surface structures with/without adsorbates (H and CO) were relaxed.

To convert DFT calculated binding energies into free energies, we added free energy corrections (zero point energies, enthalpic and entropic contributions) for adsorbed CO and H, and gaseous CO and H₂. Harmonic oscillator approximation and ideal gas approximation were used to calculate the free energy corrections for adsorbates and gaseous molecules, respectively, as implemented in Atomic Simulation Environment (ASE).⁷ The corrections values for H and CO binding free energies are collectively +0.24 eV and +0.50 eV, respectively ($\Delta G_{H*} = \Delta E_{H*} + 0.24$, $\Delta G_{CO*} = \Delta E_{CO*} + 0.50$), where ΔE_{H*} and ΔE_{CO*} are calculated as $\Delta E_{H*} = E(H^*) - E(*) - 1/2E(H_2)$ and $\Delta E_{CO*} = E(CO^*) - E(*) - E(CO)$.¹

Computational Resources

We used Fireworks to manage automatic high-throughput calculations. Arjuna cluster at Carnegie Mellon University was mainly utilized for these computations, which have 70 CPU nodes, each with 128 GB memory and 56 cores. After generating all surface structures, we performed VASP optimization once for each job and collected successfully converged jobs. “Average core-hours” for each job are 32.98 hours, which are calculated as “average real time (2.56 hours) × “average number of cores”, where the second term varies with jobs. The total number of converged calculations is approximately 28,000 considering 21,000 slab+H* structures and 7,000 slab structures. In total, the estimated total core hours are 923,440 hours. Note that failed jobs are not included in this estimation.

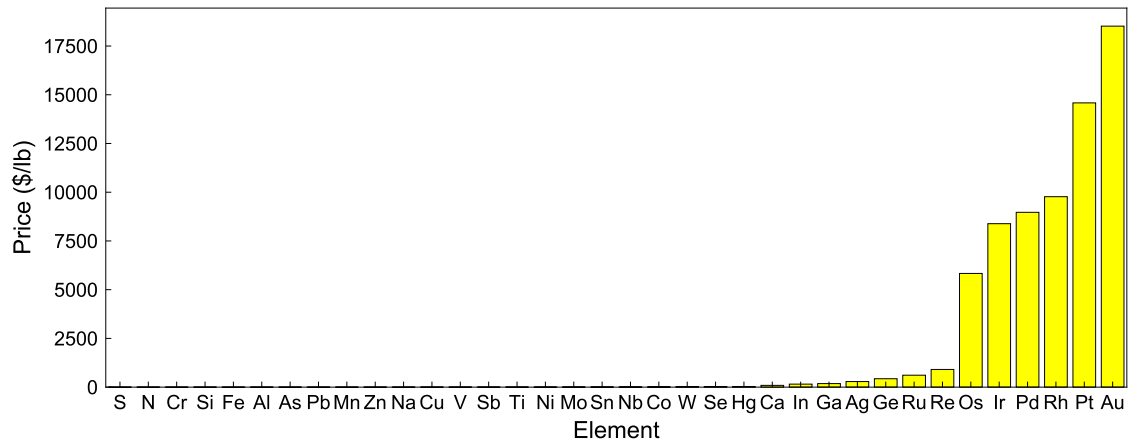


Figure S1: Prices of elements in ascending order.

Table S1: Prices of elements collected from "minerals.usgs.gov"

Element	Price (\$/lb)
Ag	286.12
Al	0.8
As	0.88
Au	18520.79
Ca	90.72
Co	11.9
Cr	0.09
Cu	2.2
Fe	0.2
Ga	181.44
Ge	430.91
Hg	26.32
In	154.22
Ir	8385.4
Mn	0.93
Mo	6.58
N	0.06
Na	1.13
Nb	9.07
Ni	4.22
Os	5833.32
Pb	0.9
Pd	8968.73
Pt	14583.3
Re	907.18
Rh	9770.81
Ru	612.5
S	0.04
Sb	3.18
Se	26
Si	0.09
Sn	7.7
Ti	3.65
V	3.1
W	22.07
Zn	0.99

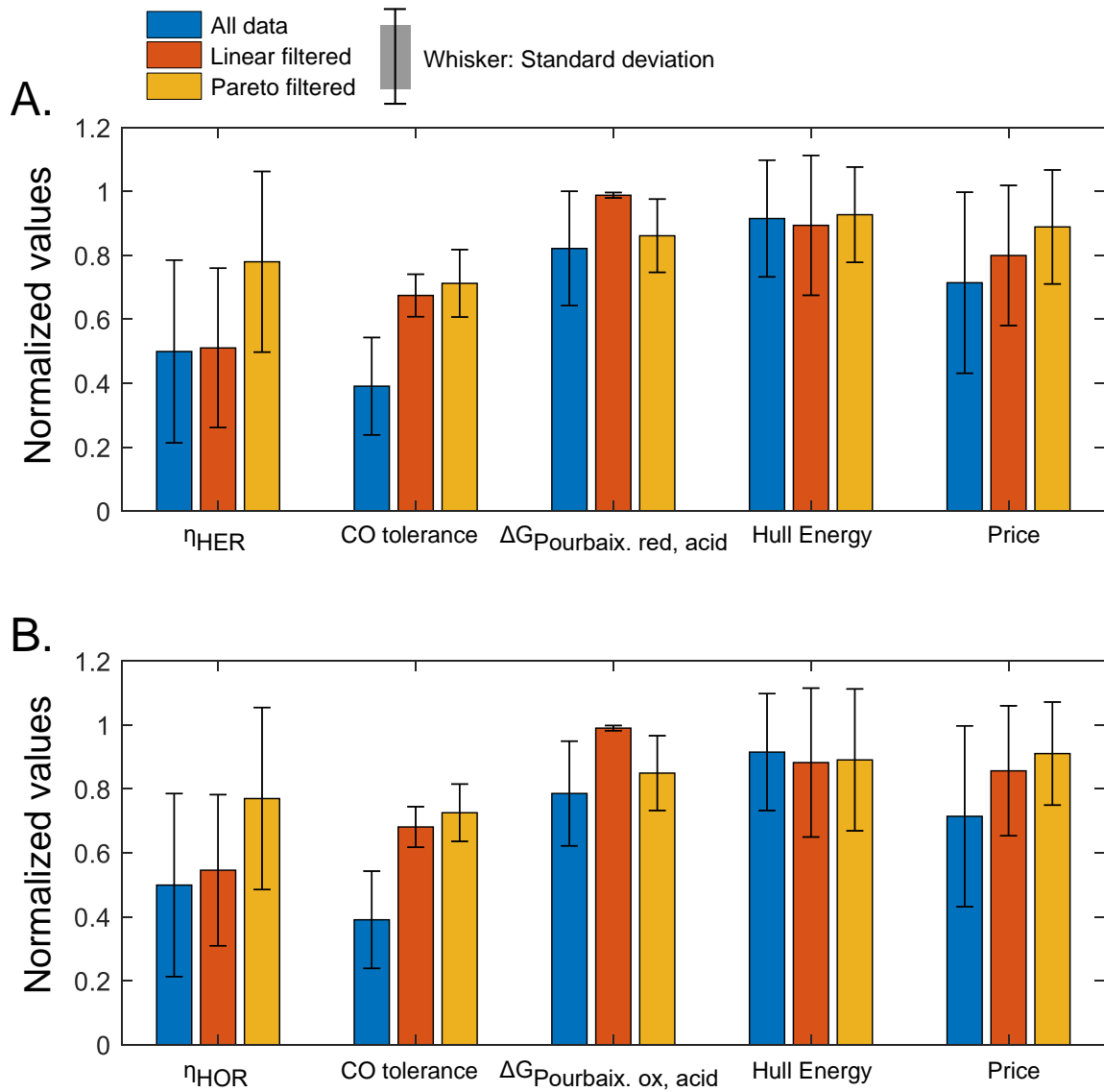


Figure S2: Statistical comparative study of all data (blue), stability-targeted linear filtered candidates (red), and multi-dimensional Pareto optimal filtered candidates (orange) for (A) HER and (B) HOR catalysts. We normalized the objective values so that values are bounded between 0 and 1. Thus, values closer to 1 represent better properties. Bars and whiskers represent mean value and standard deviation, respectively.

Table S2: Summary of promising acid stable HER catalysts and their properties (Linear filtered).

MPIID	ΔG_{H^*} (eV)	ΔG_{CO^*} (eV)	Binding Site Coordination	Price (\$/lb)	Elements	Miller Index	$\Delta G_{Pourbaix,ox,acid}$ (eV/atom)	E above hull (eV)
mp-9835	0.13	0.28	Sb	4.88	Co, Sb	[0, 1, 2]	0.06	0.01
mp-9835	0.05	0.50	Co	4.88	Co, Sb	[2, 1, 0]	0.06	0.01
mp-675626	0.08	0.10	Se	14.96	As, Cu, Se	[1, 0, 2]	0.07	0.00
mp-675626	-0.08	0.51	As	14.96	As, Cu, Se	[1, 0, 1]	0.07	0.00
mp-11658	0.16	0.70	Se	15.23	Cu, Se, Sn	[2, 0, 1]	0.05	0.01
mp-22811	0.06	0.15	Se	65.28	Cu, In, Se	[1, 1, 1]	0.06	0.00
mp-29249	0.02	-0.03	Se	147.52	As, Ge, Se	[0, 0, 1]	0.03	0.00
mp-10074	0.04	0.49	Se	153.55	Ge, Se	[1, 0, 1]	0.07	0.02
mp-766	0.05	-0.15	As	247.25	As, Ru	[1, 2, 0]	0.00	0.00
mp-2695	-0.16	0.51	Os	2560.11	Os, Sb	[0, 1, 2]	0.01	0.00
mp-2682	0.17	0.49	Rh	2904.65	Rh, Sb	[2, 1, -1]	0.09	0.00
mp-2682	0.19	0.43	Rh	2904.65	Rh, Sb	[2, 1, -1]	0.09	0.00
mp-2455	0.08	0.45	As	3263.43	As, Os	[1, 1, 0]	0.00	0.00
mp-1247	-0.07	0.42	Ir	3700.84	Ir, Sb	[1, 0, 0]	0.00	0.00
mp-1247	-0.10	0.42	Ir	3700.84	Ir, Sb	[1, 1, 1]	0.00	0.00
mp-20466	-0.07	0.58	Ir	4500.69	Ir, Sn	[1, 0, 0]	0.08	0.00
mp-2444	-0.12	0.08	Ga	5897.76	Ga, Rh	[1, 0, 0]	0.04	0.00
mp-12086	0.14	0.12	Pt	7376.78	Cu, Pt	[2, 1, 1]	0.05	0.00
mp-863709	-0.12	0.23	Ir	8595.19	Ir, Rh	[1, 1, 0]	0.00	0.00
mp-19856	-0.12	-0.17	Pt	9069.27	Pt, Sn	[1, 1, 1]	0.00	0.00
mp-571060	0.05	0.52	Pt	10406.06	In, Pt	[1, 1, -1]	0.06	0.05
mp-1025366	0.17	0.25	Pt	12641.67	Pt, Sb, Si	[1, 0, 1]	0.09	0.02

Table S3: Summary of promising acid stable HOR catalysts and their properties (Linear filtered).

MPIID	ΔG_{H^*} (eV)	ΔG_{CO^*} (eV)	Binding Site Coordination	Price (\$/lb)	Elements	Miller Index	$\Delta G_{Pourbaix,ox,acid}$ (eV/atom)	E above hull (eV)
mp-675626	-0.08	0.51	As	14.96	As, Cu, Se	[1, 0, 1]	0.02	0.00
mp-675626	0.08	0.10	Se	14.96	As, Cu, Se	[1, 0, 2]	0.02	0.00
mp-11658	0.16	0.70	Se	15.23	Cu, Se, Sn	[2, 0, 1]	0.02	0.01
mp-22811	0.06	0.15	Se	65.28	Cu, In, Se	[1, 1, 1]	0.03	0.00
mp-12086	0.14	0.12	Pt	7376.78	Cu, Pt	[2, 1, 1]	0.05	0.00

Table S4: Summary of promising acid stable HER catalysts and their properties (Pareto optimal filtered).

MPID	ΔG_{H^*} (eV)	ΔG_{CO^*} (eV)	Binding Site Coordination	Price (\$/lb)	Elements	Miller Index	$\Delta G_{Pourbaix,ox,acid}$ (eV/atom)	E above hull (eV)
mp-849086	-0.01	-0.07	S	1.12	Cu, S	[2, 0, 1]	0.93	0.00
mp-5305	-0.01	-0.09	As	1.21	As, Cu, S	[2, 1, 2]	0.53	0.00
mp-2291	-0.01	0.83	Si	2.2	Ni, Si	[1, 1, 1]	1.4	0.00
mp-862691	-0.01	0.42	Co	4.48	Al, Co, Fe	[2, 1, 0]	1.34	0.00
mp-2182	0.01	0.51	As	5.06	As, Sn	[1, 1, 1]	0.24	0.01
mp-22631	0.16	0.85	N	10.64	Co, N	[2, 1, 1]	1.32	0.00
mp-11658	0.16	0.7	Se	15.23	Cu, Se, Sn	[2, 0, 1]	0.05	0.01
mp-13133	-0.02	0.47	Se	16.75	Cu, Se, Sn	[1, 1, 0]	0.09	0.07
mp-1018059	0	0.34	Ga	68.09	Ga, Sb	[2, 1, 1]	0.6	0.01
mp-29249	0.02	-0.03	Se	147.52	As, Ge, Se	[0, 0, 1]	0.03	0.00
mp-10074	0.04	0.49	Se	153.55	Ge, Se	[1, 0, 1]	0.07	0.02
mp-5342	-0.02	0.35	S	180.03	Ag, Ga, S	[0, 0, 1]	0.61	0.00
mp-30660	-0.03	0.53	Ga	2236.54	Ga, Pd	[1, 1, 0]	0.32	0.00
mp-570844	-0.18	1.48	Os	2873.38	Ga, Os	[1, 1, 0]	0.55	0.00
mp-630976	-0.04	0.63	Ir	3102.34	In, Ir	[1, 0, 1]	0.41	0.00
mp-20466	-0.07	0.58	Ir	4500.69	Ir, Sn	[1, 0, 0]	0.08	0.00
mp-2287	0.07	0.64	Si	7675.92	Rh, Si	[1, 1, -2]	1.05	0.02
mp-11152	0	0.2	Si	8249.11	Pt, Sb, Si	[0, 0, 1]	1.03	0.00
mp-510438	-0.01	0.43	Pt	9237.36	In, Pt	[2, 2, 1]	0.12	0.02

Table S5: Summary of promising acid stable HOR catalysts and their properties (Pareto optimal filtered).

MPIID	ΔG_{H^*} (eV)	ΔG_{CO^*} (eV)	Binding Site Coordination	Price (\$/lb)	Elements	Miller Index	$\Delta G_{Pourbaix,ox,acid}$ (eV/atom)	E above hull (eV)
mp-849086	-0.01	-0.07	S	1.12	Cu, S	[2, 0, 1]	0.65	0.00
mp-2291	-0.01	0.83	Si	2.2	Ni, Si	[1, 1, 1]	2.08	0.00
mp-862691	-0.01	0.42	Co	4.48	Al, Co , Fe	[2, 1, 0]	1.49	0.00
mp-2182	0.01	0.51	As	5.06	As, Sn	[1, 1, 1]	1.21	0.01
mp-22631	0.16	0.85	N	10.64	Co, N	[2, 1, 1]	1.42	0.00
mp-675626	-0.08	0.51	As	14.96	As, Cu , Se	[1, 0, 1]	0.02	0.00
mp-11658	0.16	0.7	Se	15.23	Cu, Se, Sn	[2, 0, 1]	0.02	0.01
mp-13133	-0.02	0.47	Se	16.75	Cu, Se, Sn	[1, 1, 0]	0.02	0.07
mp-22811	0.06	0.15	Se	65.28	Cu, In, Se	[1, 1, 1]	0.03	0.00
mp-1018059	0	0.34	Ga	68.09	Ga, Sb	[2, 1, 1]	1.8	0.01
mp-674493	0.01	0.48	S	85.62	In, Ni, S	[0, 0, 1]	0.43	0.09
mp-984714	0	0.24	S	143.96	Ag, As, S	[1, 2, 1]	0.67	0.01
mp-10074	0.04	0.49	Se	153.55	Ge, Se	[1, 0, 1]	0.19	0.02
mp-5342	-0.02	0.35	S	180.03	Ag, Ga, S	[0, 0, 1]	0.5	0.00
mp-30660	-0.03	0.53	Ga	2236.54	Ga, Pd	[1, 1, 0]	0.8	0.00
mp-570844	-0.18	1.48	Os	2873.38	Ga, Os	[1, 1, 0]	1.15	0.00
mp-630976	-0.04	0.63	Ir	3102.34	In, Ir	[1, 0, 1]	1.01	0.00
mp-20466	-0.07	0.58	Ir	4500.69	Ir, Sn	[1, 0, 0]	0.59	0.00
mp-11152	0	0.2	Si	8249.11	Pt, Sb, Si	[0, 0, 1]	1.69	0.00
mp-510438	-0.01	0.43	Pt	9237.36	In, Pt	[2, 2, 1]	0.65	0.02

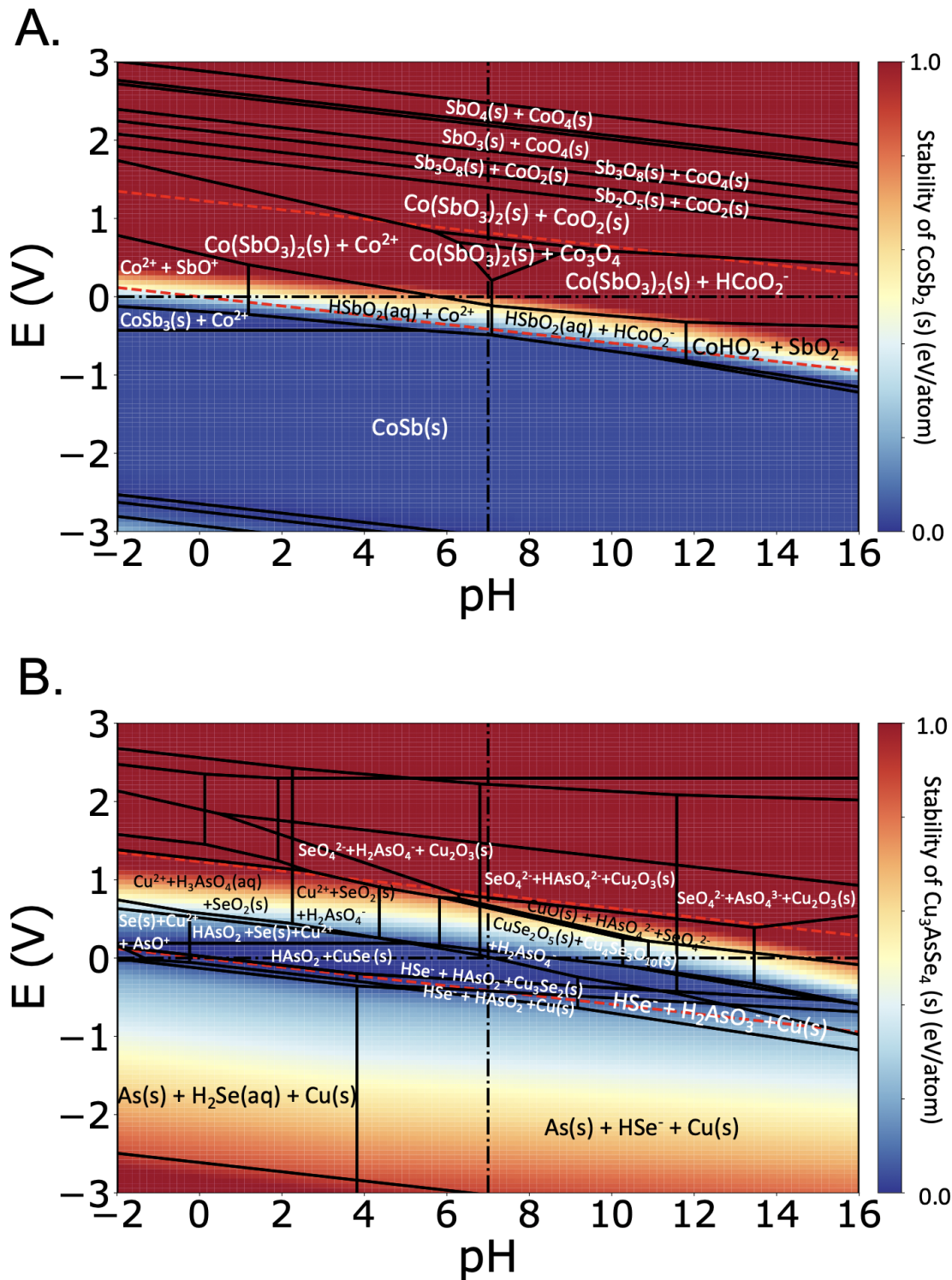


Figure S3: The Pourbaix diagrams of promising candidates for (A) HER (CoSb_2) and (B) HOR (Cu_3AsSe_4). The relative electrochemical stability of two promising candidates are visualized as a heat map, where blue area indicates higher stability.

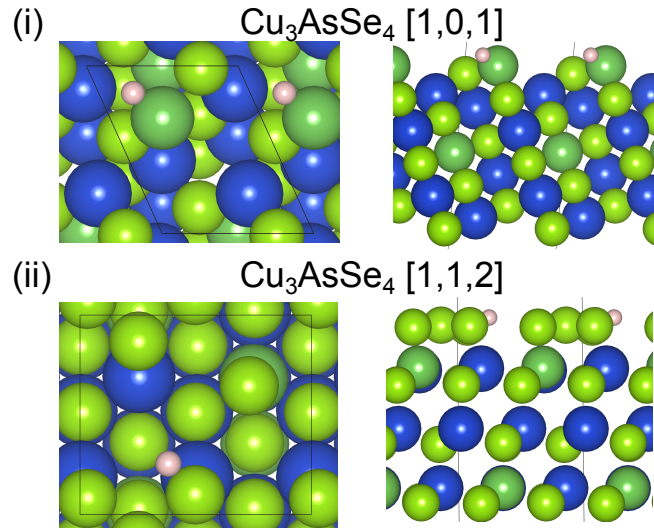
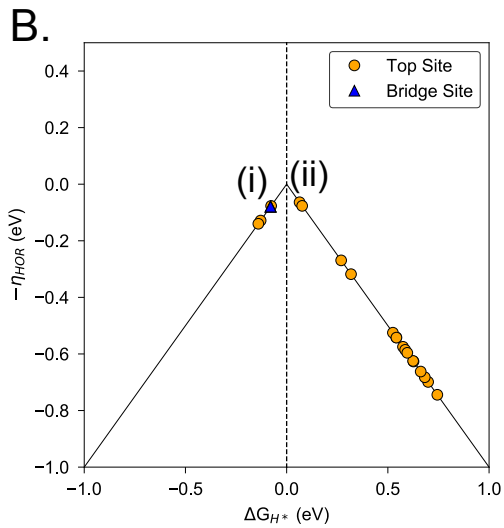
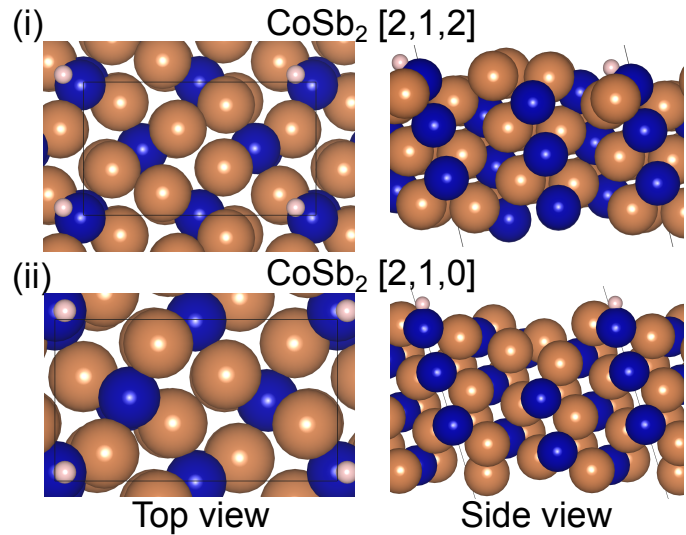
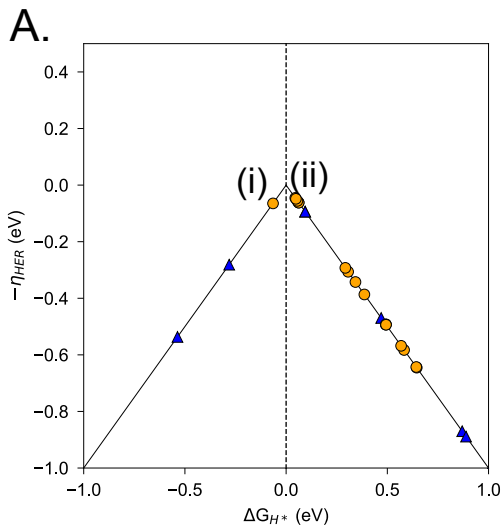


Figure S4: Volcano plots of (A) HER (CoSb_2) and (B) HOR (Cu_3AsSe_4), and top/side views of their most active sites. Color codes: navy (Co), orange (Sb), light green (Se), dark green (As), blue (Cu), white (H).

Supplementary Note

For the promising candidate materials for HER and HOR, we present their Pourbaix diagrams and volcano plots in Figure S2 and S3, respectively. The calculated electrochemical stabilities under the reaction conditions of CoSb_2 and Cu_3AsSe_4 are 0.06 and 0.02 eV/atom, and the most stable phases under the reaction conditions are predicted to be $\text{CoSb}_3(\text{s}) + \text{Co}^{2+}$ and $\text{CuSe}(\text{s}) + \text{HAsO}_2(\text{aq})$, respectively. 0.06 and 0.02 eV/atom of the electrochemical stabilities of CoSb_2 and Cu_3AsSe_4 indicate weak driving forces to decompose into the most stable phases.

Figure S3 shows volcano plots to evaluate the catalytic activity for HER and HOR based on ΔG_{H^*} . All calculated DFT data (25 sites for CoSb_2 and 24 sites for Cu_3AsSe_4) are taken from GASpy database.¹ For both materials, there are several binding sites with on-top adsorption configurations and ΔG_{H^*} close to 0.00 eV, where their surface structures are visualized. For CoSb_2 , all the active sites are either Co top site or Co-Co bridge sites, while Sb containing sites are too weakly binding H^* . Among them, Co top site binding showed the optimal ΔG_{H^*} close to 0 eV. For Cu_3AsSe_4 , both As and Se top site binding exhibited ΔG_{H^*} close to 0 eV.

References

- (1) Tran, K.; Ulissi, Z. W. Active learning across intermetallics to guide discovery of electrocatalysts for CO₂ reduction and H₂ evolution. *Nat. Catal.* **2018**, *1*, 696.
- (2) Jain, A.; Ong, S. P.; Hautier, G.; Chen, W.; Richards, W. D.; Dacek, S.; Cholia, S.; Gunter, D.; Skinner, D.; Ceder, G.; Persson, K. Commentary: The Materials Project: A materials genome approach to accelerating materials innovation. *APL Mater.* **2013**, *1*, 011002.
- (3) Kresse, G., et al. G. Kresse and J. Furthmüller, Comput. Mater. Sci. 6, 15 (1996). *Comput. Mater. Sci.* **1996**, *6*, 15.
- (4) Kresse, G.; Hafner, J. Ab initio molecular dynamics for open-shell transition metals. *Phys. Rev. B* **1993**, *48*, 13115.
- (5) Hammer, B.; Hansen, L. B.; Nørskov, J. K. Improved adsorption energetics within density-functional theory using revised Perdew-Burke-Ernzerhof functionals. *Phys. Rev. B* **1999**, *59*, 7413.
- (6) Kresse, G.; Joubert, D. From ultrasoft pseudopotentials to the projector augmented-wave method. *Phys. Rev. B* **1999**, *59*, 1758.
- (7) Larsen, A. H.; Mortensen, J. J.; Blomqvist, J.; Castelli, I. E.; Christensen, R.; Dułak, M.; Friis, J.; Groves, M. N.; Hammer, B.; Hargus, C., et al. The atomic simulation environment—a Python library for working with atoms. *J. Phys. Condens. Matter* **2017**, *29*, 273002.